Transition metal interaction and Ni-Fe-Cu-Si phases in silicon

M. Heuer,[a] T. Buonassisi,[b] A. A. Istratov,[c] and M. D. Pickett
Department of Materials Science and Engineering, University of California, Berkeley and Materials Science Division, Lawrence Berkeley National Laboratory, Berkeley, California 94720

M. A. Marcus
Advanced Light Source, Lawrence Berkeley National Laboratory, Berkeley, California 94720

A. M. Minor
National Center for Electron Microscopy, Lawrence Berkeley National Laboratory, Berkeley, California 94720

E. R. Weber[d]
Department of Materials Science and Engineering, University of California, Berkeley and Materials Science Division, Lawrence Berkeley National Laboratory, Berkeley, California 94720

In the present article we characterize several intermetallic phases of the Cu-Ni-Fe-Si system found as precipitates in the misfit dislocation layer of intentionally contaminated and slowly cooled $Si_{1-x}Ge_x$/Si-heterostructures. The clusters showed a characteristic phase speciation into a Cu-rich part similar to Cu_3Si and an Fe-Ni-Cu-Si phase similar to $NiSi_2$. It is suggested that the precipitate formation of the investigated intermetallic silicides involves a homogeneous precursor phase at higher temperatures that later decomposes into the observed phases. Our results indicate that chemical reactions between metals and silicon during precipitation may reduce the lattice mismatch compared to single-metal precipitates, rendering mixed-metal-silicide precipitates more stable and energetically favorable. [DOI: 10.1063/1.2748346]

I. INTRODUCTION

About 91% of solar cells currently produced are based on crystalline silicon, the majority being of multicrystalline silicon (mc-Si).[1] Depending on the technology the silicon cost may be up to 25% of the cost of solar cells. Furthermore, the available amount of electronic-grade silicon cannot cover the feedstock demands of the photovoltaic (PV) industry and the use of electronic-grade silicon is not cost efficient. Therefore, the PV industry is considering the possibility of using cheaper and dirtier materials. These materials are known as solar-grade silicon (SoG-Si),[2,3] and have a relatively high transition metal content, which is considered a major culprit for losses in solar cell efficiencies.[4,5]

Since the majority of conventional solar cell technologies are poorly suited for solar-grade silicon, and the idea of using dirtier silicon for PV attracted renewed attention, one of the central problems that remains to be solved is the development of an effective defect engineering process for lower-purity mc-Si.

It is known that the electrical properties of silicon are not directly related to the total metal content, since metals can occur in different active forms within the material, i.e., homogeneously solved as well as locally concentrated in precipitates. Hence, the chemical states of these metals are of great importance for the electrical properties.[4,5]

The concept of metal defect engineering recently suggested by Buonassisi *et al.*[6] is based on reducing the detrimental impact of metals in solar cells by changing their spatial distribution or chemical state to achieve the lowest possible recombination activity of metal silicide clusters.

Common solar cell materials are not contaminated with just one metal species, but with a variety of transition metals,[7,8] so there may be a chemical interaction between the different contaminants leading to different characteristics as for systems with only one or one dominant contamination species.

Such interaction was recently confirmed by the identification of silicide clusters in mc-Si containing Cu, Ni, and Fe at the same time. It was found that a silicide with composition of $Ni_{0.82}Fe_{0.21}Cu_{0.02}Si_{1.94}$ crystallizes in a structure similar to $NiSi_2$ but with mixed occupancies of Fe on the Ni- and Cu on the Si- site.[9]

It is instrumental to understand the properties and the mechanisms of formation of multimetal silicides because, depending on their recombination properties, they may either be undesired species whose formation should be suppressed, or efficient internal gettering sinks for transition metals. Likewise, the gettering and hydrogen passivation of transition metal clusters depends on their chemical state and may be different for intermetallic silicides than for single-metal silicides.

In the present article we characterize several intermetallic phases of the Cu-Ni-Fe-Si system found as precipitates in

[a]Author to whom correspondence should be addressed; Present address: University of Leipzig, Scharnhorststraße 20, 04275 Leipzig, Germany; Electronic mail: m.heuer@uni-leipzig.de
[b]Present address: Massachusetts Institute of Technology, Cambridge, MA 02139–4307.
[c]Present address: Siltronic Corp., 7200 NW Front Ave., M/S 10, Portland, OR 97210.
[d]Present address: Fraunhofer Institute for Solar Energy Systems, 79110 Freiburg, Germany.

"as grown" mc-Si (Ref. 10) and intentionally contaminated model samples. Hereby, we employ synchrotron based micro- and nanoprobe techniques as well as transmission electron microscopy (TEM), energy dispersive x-ray spectroscopy (EDS) on focused ion beam (FIB) prepared samples.

II. MATERIAL

Two sample types were used in this study including $Si_{1-x}Ge_x$/Si samples containing a defined layer of misfit dislocations and Cu-Ni-Fe-Si alloys. The $Si_{1-x}Ge_x$/Si samples were used for their controlled nucleation sites within the misfit dislocation layer and were intentionally contaminated with Ni, Fe, and Cu by scratching with a wire of the respective element (on the back side of the samples, away from the misfit dislocation layer), annealed at 1100 °C for 35 min (corresponding to concentrations of Fe $\sim 2.9\times10^5$ cm^{-3}, Ni $\sim 8.4\times10^{17}$ cm^{-3}, and Cu $\sim 1.9\times10^8$ cm^{-3}) and then "slow cooled" within an hour. One of the $Si_{1-x}Ge_x$/Si samples was quenched in silicone oil to freeze in early stages of the precipitate growth.

The alloys used as reference samples were synthesized by melting mixtures of Ni, Fe, and Cu in an arc furnace under an Ar atmosphere and then solidifying from the melt within approximately 5 min.

III. EXPERIMENT

The synchrotron source utilized throughout this study was the Advanced Light Source (ALS) at Lawrence Berkeley National Laboratory. At ALS Beamline 10.3.2,[11] a state-of-the-art analytical x-ray microprobe can achieve a spot size of 7×5 μm^2 using an ultrabright x-ray beam (10^{10} photons/s).

With the beam conditions described above, precipitates a few hundred nanometers in diameter can be realistically detected. More details about the operational principles and detection limits of the μ-XRF technique can be found elsewhere.[4,12,13]

Precipitate-containing regions of the $Si_{1-x}Ge_x$/Si model samples were prepared for TEM analysis using a dual-beam FIB system at the National Center for Electron Microscopy, Berkeley (Strata 235, FEI), which contained both a focused gallium ion beam and a conventional field-emission scanning electron (FESEM) column. The ion beam was operated at 30 kV with varying beam current ranging from 20 000 pA down to 100 pA as the electron-transparent portion of the sample became thinner. Successive steps of 20 000, 1000, 500, 300, and 100 pA were employed. The initial high current (20 000 pA) was necessary to eliminate damaged near-surface layers from the prethinning procedures and for rapid early-stage milling.

An elemental mapping of bigger precipitates (1–2 μm diameter) was carried out using the integrated EDS system of the Strata 235 dual-beam FIB.

After the milling, TEM studies, specifically bright-field imaging and selected area electron diffraction (SAED), were performed on the thinned areas using a JEOL 3010 TEM at the National Center for Electron Microscopy, Berkeley, operated at 300 kV.

The alloys were characterized using x-ray diffraction (XRD) on a Seifert XRD3000 diffractometer (30 mA/40 kV; Bragg-Brentano geometry) equipped with a graphite (002) diffracted-beam monochromator and a scintillation detector. A powder diffraction pattern was recorded in the range of 5°–100° 2θ with a step size of 0.05° 2θ and 2s/step. EDS mapping at these samples was carried out using the Strata 235 dual-beam FIB system.

Differential scanning calorimetry (DSC) was carried out using a calorimeter constructed at our laboratory and suited for measurements up to 1300 °C. Reproducible results were obtained on powder samples (typical weight 1 g) in open silica capsules. Al_2O_3 was used as reference material. To guarantee the identity of thermal conditions for the sample and the reference material, both were placed into a high-temperature steel clamp. During the measurement the sample was heated at a constant rate of 2–3 K/min. The temperatures of the sample and the reference material were determined with Pt/90% Pt-10% Rh thermocouples. The difference signal between the sample and reference material temperature was amplified and registered together with the temperature signal itself. For each peak in the difference signal, a phase-transition temperature was determined from the baseline intercept of the tangent to the leading edge of the peak. The accuracy of the transition temperatures was ±2 K. Calibration of the temperature scale was achieved by recording the solid-state phase transitions and melting points of K_2SO_4 (585 and 1069 °C), NaCl (801 °C), and gold (1064 °C).

IV. RESULTS AND DISCUSSION

A. Investigations on $Si_{1-x}Ge_x$/Si samples

In our previous work, μ-XRF and μ-EXAFS were used to identify and describe a Ni-Fe-Cu-silicide compound forming in Si simultaneously contaminated with multiple metal species. The atomic structure was determined by computer modeling of the spectra and can be described as a CaF_2 type with mixed occupancies of Fe and Ni on the Ca site, and Cu and Si on the F site.[9]

Conventional μ-XRF with medium resolution (spot size 5×7 μm^2) on $Si_{1-x}Ge_x$/Si samples shows precipitates containing Cu, Ni, and Fe (Fig. 1) but does not distinguish between simple coprecipitation and formation of more complex intermetallic phases.

Therefore, additional investigations with higher spatial resolution are necessary; thus, FIB preparation and EDS were utilized to study the phase speciation of bigger clusters and to prepare samples for TEM. Hereby $Si_{1-x}Ge_x$/Si heterostructures were used to obtain precipitates at controlled nucleation sites within the misfit dislocation network in a defined layer of the sample. Figure 2 shows one of the investigated clusters consisting of a copper-rich silicide and a Ni-Cu-silicide. The precipitate morphology can be described as a hexagonal-shaped platelet, with a diameter of 2 μm, on a {111} plane. The particle is divided into two sections, suggesting a phase separation after the precipitate was formed.

As shown by Buonassisi *et al.*, in some bigger clusters found in slow-cooled multicrystalline float zone (mc-FZ) material, μ-XRF with high resolution indicates a phase spe-

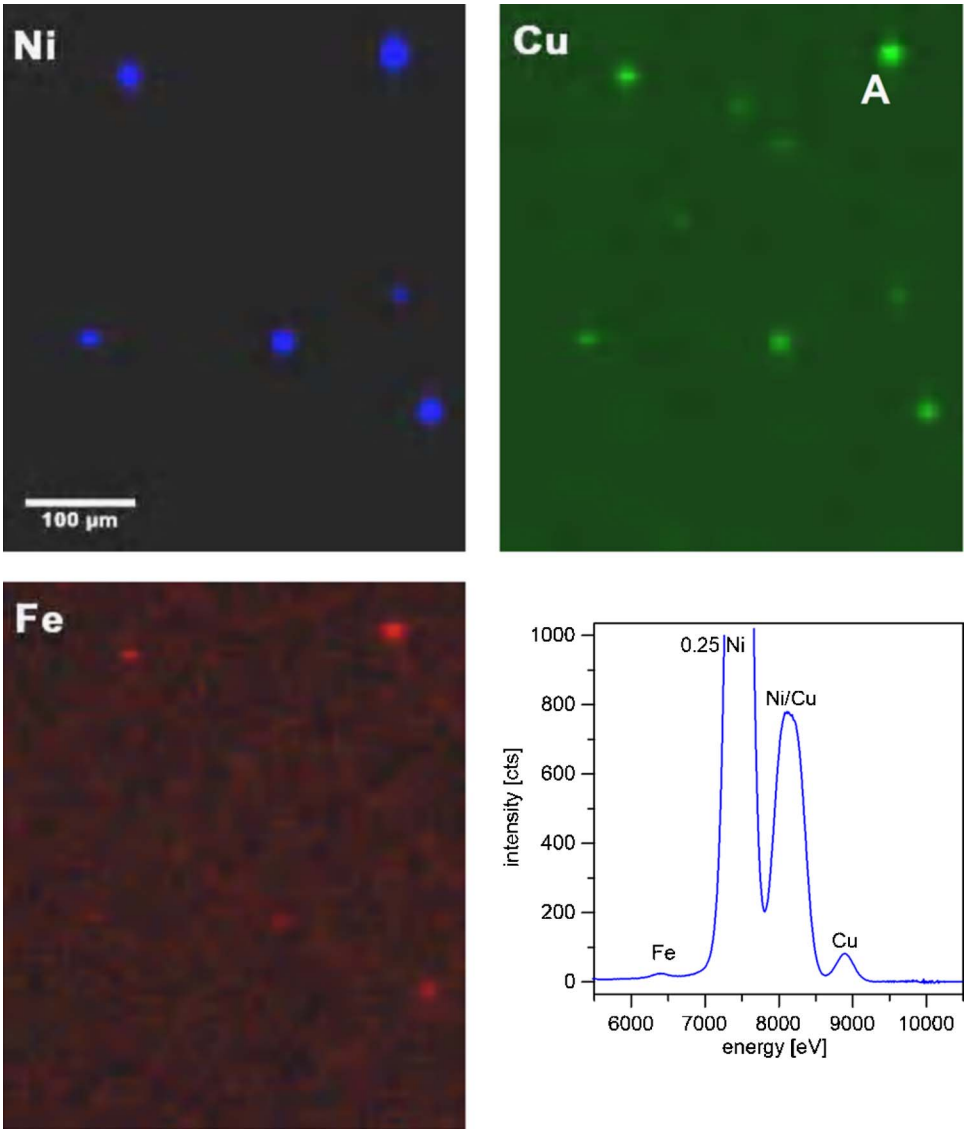

FIG. 1. μ-XRF maps of precipitates in intentionally contaminated $Si_{1-x}Ge_x$/Si samples containing Cu, Ni, and Fe. The lower right figure shows a background subtracted μ-XRF point spectrum of particle "A."

ciation into a Cu-rich phase and a Ni-Fe-Cu-Si phase.[10] In this work, a phase separation similar to the FZ samples was found but with no or lower iron contents of the involved phases.

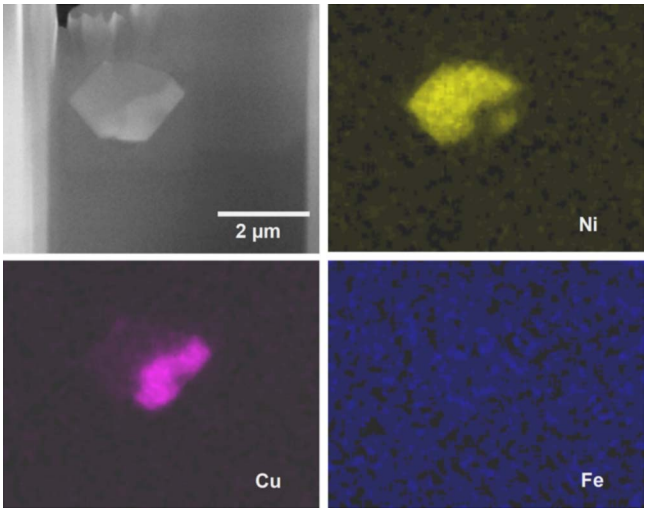

FIG. 2. SEM image and EDS maps of a precipitate in $Si_{1-x}Ge_x$/Si showing speciation into a Cu-rich phase and a Ni-Cu-Si phase.

The EDS measurements showed that the copper-rich phase of this sample has a composition of $Cu_{0.733(4)}Ni_{0.017(1)}Si_{0.202(1)}Ge_{0.049(1)}$, which could be a Ni-bearing Cu_3Si with some Ge from the $Si_{1-x}Ge_x$/Si layer. The composition of the Ni-Cu-silicide forming the other part of the precipitate can be given by $Ni_{0.309(1)}Cu_{0.029(1)}Ge_{0.079(1)}Si_{0.578(1)}$, which is close to $NiSi_2$. In other precipitates, small amounts of iron were found leading to a composition of $Ni_{0.83(1)}Cu_{0.15(1)}Fe_{0.01(1)}Ge_{0.03(1)}Si_2$, which is close to the reference material used for the EXAFS study.[9]

SAED of the different precipitate parts compared with calculated SAD patterns confirmed a $NiSi_2$ structure for Ni-rich part of the precipitate (see Fig. 3). Since η''-Cu_3Si has a complicated superstructure (stacking fault structure) at room temperature,[14] the identification by comparison with calculated SAD patterns was more difficult, yet these confirm a close structural relation of the investigated copper-rich parts of the precipitates with Cu_3Si (see Fig. 3).

Thus, it was possible to index and identify the substructure reflections using the η-Cu_3Si structure model, but not possible to index the superstructure reflections. These addi-

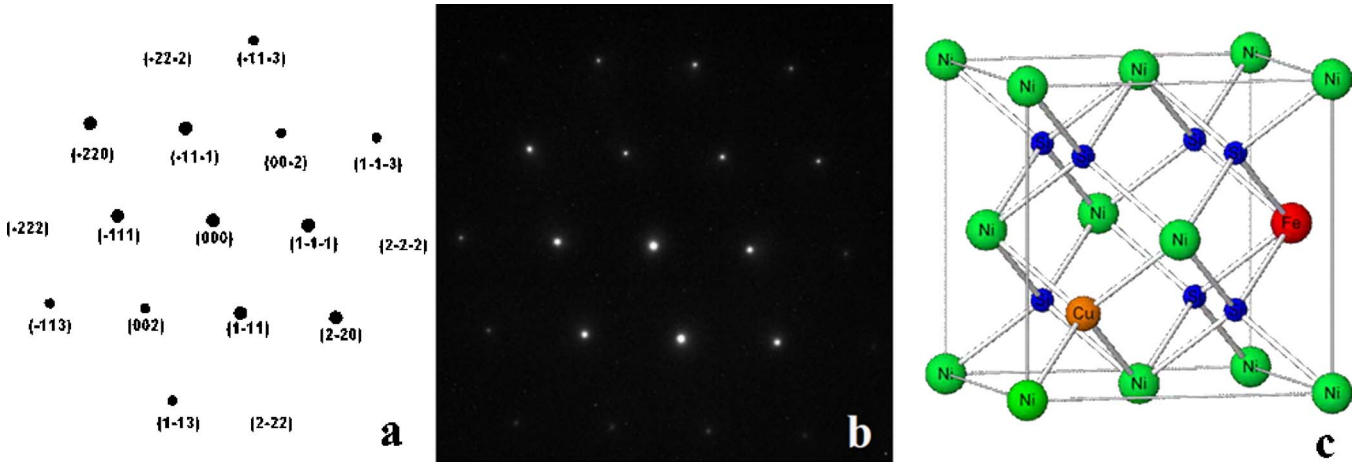

FIG. 3. simulated (a) and measured (b) SAD pattern on the nickel-rich part of the precipitate in Fig. 2, confirming a $NiSi_2$ structure (c) of the precipitate part.

tional reflections suggest a superstructure with 3 times higher translation period in the [11–1] direction and 4 times higher translation period in [001] relating to the η-Cu_3Si structure [Fig. 4(c)]. η-Cu_3Si is the high-temperature modification of Cu_3Si, and the low-temperature modification η'' which is observed in TEM at room temperature can be described as superstructure of η-Cu_3Si.[14]

The quenched $Si_{1-x}Ge_x$/Si sample was examined by means of TEM to obtain information on the early precipitation states of Fe-Ni-Cu-contaminated samples. As shown in Fig. 5, there is a clear correlation of precipitates and dislocations, and as expected, the misfit dislocation network of S $Si_{1-x}Ge_x$/Si heterostructures can be used as a preferred nucleation site.

Again, the precipitates can be described as hexagonal shaped platelets on {111} planes, which are much smaller and have diameters from 40 to 200 nm [Fig. 5(a)]. The orientation of matrix and precipitates is given in Fig. 5(b).

Furthermore, Fig. 5(a) shows some of these precipitates decorating 60° dislocations of the first dislocation layer close to the $Si_{1-x}Ge_x$/Si interface. The following dislocation layers far from the $Si_{1-x}Ge_x$/Si interface did not show any precipitate decoration.

EDS measurements on such particles confirm a uniform composition of approximately $Ni_{0.80(5)}Cu_{0.17(5)}Fe_{0.03(5)}Ge_{0.02(5)}Si_{1.98(5)}$. A typical EDS spectrum is shown in Fig. 6. Here again, a small Ge content originates from the $Si_{1-x}Ge_x$ layer, and the precipitate is a Cu-containing $NiSi_2$ phase with a very small Fe content. There were no signs of phase separation as in the slowly cooled samples, and no coprecipitation of different phases was detected.

B. Investigations on Fe-Ni-Cu-Si alloys

Since very little is known about the possible phases in the Fe-Ni-Cu-Si quaternary system, different alloys of this system were investigated as a reference. XRD and EDS analysis of a sample with an initial weight of $Cu_{0.374}Ni_{0.170}Fe_{0.021}Si_{0.436}$ revealed the presence of $(Cu, Ni)_3Si$ and $(Ni, Cu, Fe)(Si, Cu)_2$ phases after solidification from the melt. The diffraction pattern in Fig. 7 indicates two dominating structures similar to Cu_3Si and $NiSi_2$, whereas the EDS measurements confirm that each set of diffraction peaks is a superposition of two structurally very similar but chemically different

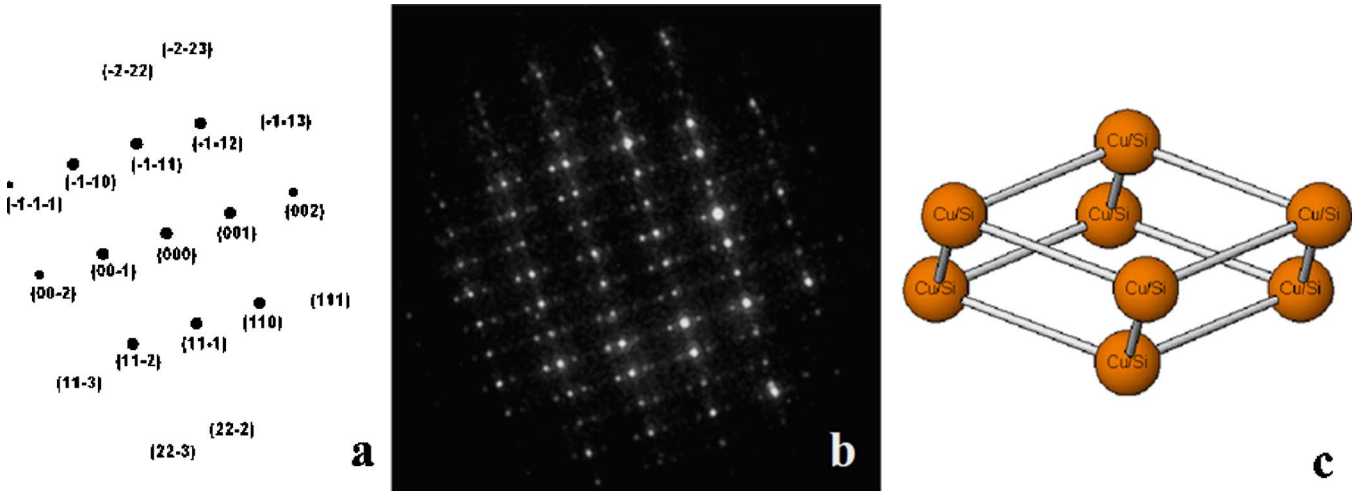

FIG. 4. Simulated (a) and measured (b) SAD pattern on the copper-rich part of the precipitate in Fig. 2, suggesting a Cu_3Si structure of the precipitate part. Note the reflection indices (a) are referring to the η-Cu_3Si structure (c) (Ref. 14).

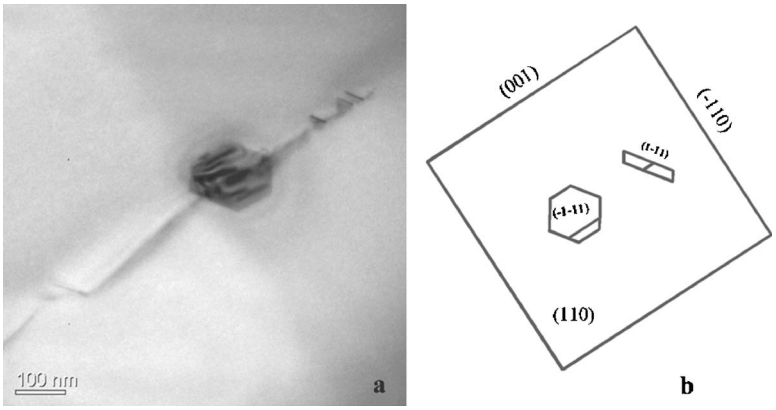

FIG. 5. Fe-Ni-Cu-silicide precipitates (a) decorating 60° dislocations in an intentionally contaminated $Si_{1-x}Ge_x$/Si heterostructure (quenched sample), orientation relation (b).

phases. Accordingly two types of Ni-bearing Cu_3Si phases, $Cu_{2.49(1)}Ni_{0.49(1)}Si_{1.00(1)}$ and $Cu_{2.95(1)}Ni_{0.13(1)}Si_{0.92(1)}$, and two types of Cu-containing $NiSi_2$ phases, $Ni_{0.88(1)}Fe_{0.13(1)}Cu_{0.09(1)}Si_{1.89(1)}$ and $Ni_{0.99(1)}Cu_{0.18(1)}Si_{1.82(1)}$, were found. SEM images of a polished section of the sample indicate that the material consists of coarse $Ni_{0.88(1)}Fe_{0.13(1)}Cu_{0.09(1)}Si_{1.89(1)}$ grains (100 μm) and a eutectic texture of the both Cu-rich phases and $Ni_{0.99(1)}Cu_{0.18(1)}Si_{1.82(1)}$ (Fig. 8).

DSC was performed during melting and resolidifying of this sample and revealed two main transition points, a first peak at 940 °C and a second at 740 °C. These DSC features have yet to be associated with phase transformations of a specific multimetal silicide phase, but compared to Si-(Cu, Ni, Fe) binary alloys, the quaternary Fe-Ni-Cu-Si system could feature eutectic points at relatively low temperatures. In an additional heating experiment, it was verified that parts of the sample were molten at 750 °C. The melting points of the pure silicides are significantly higher and are given with 1220 °C, 1090 °C, and 859 °C for $FeSi_2$, $NiSi_2$, and Cu_3Si, respectively.

V. CONCLUSIONS

Intermetallic-silicide clusters containing Cu, Ni, and Fe of up to 1–2 μm in size were found in intentionally contaminated and slow cooled $Si_{1-x}Ge_x$/Si heterostructures. These samples were used as model materials to study the clustering of multiple-metal precipitates observed also in as grown mc-silicon for solar cell production.[10]

The samples contained clusters showing a characteristic phase speciation into a Cu-rich part similar to Cu_3Si and Fe-Ni-Cu-Si phase similar to $NiSi_2$. Hereby, SEM/EDS examinations revealed that such clusters, although consisting of two different phases, show one uniform morphology.

This leads to the conclusion that the phase separation is a secondary effect and takes place after the precipitate has formed. Thus, it is possible that at higher temperatures, a homogeneous precipitate starts to form, which then decomposes into the detected species. Considering the fact that multiternary systems like Fe-Ni-Cu-Si might contain low melting eutectics, it is even conceivable that the first stage of the forming precipitate is a liquid inclusion.

Another important aspect is that the two parts of these huge clusters are single-crystalline precipitates that are intergrown with the silicon matrix in a systematic orientation relation. It suggests that the formation of mixed intermetallic silicides has a reduced lattice mismatch compared with single-metal precipitates and is therefore more stable and energetically favorable.

An intentionally contaminated $Si_{1-x}Ge_x$/Si heterostructure, which was annealed and then quenched, showed much smaller precipitates of an Fe-Ni-Cu-Si phase similar to

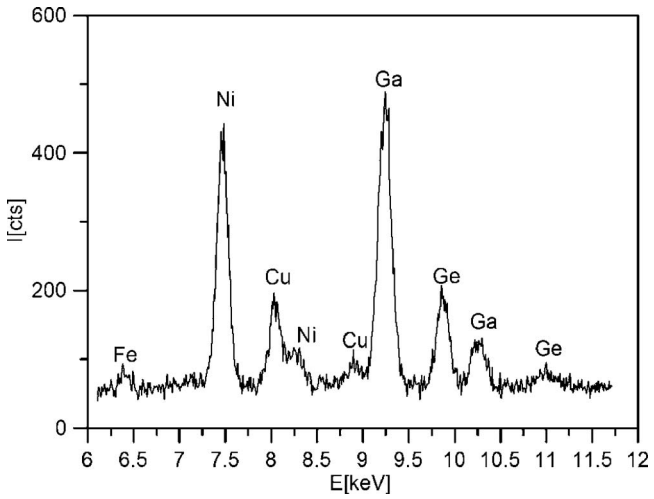

FIG. 6. Typical TEM-EDS spectrum of an Fe-Ni-Cu-silicide precipitate in an intentionally contaminated $Si_{1-x}Ge_x$/Si heterostructure (quenched sample). Note the Ga content is from FIB milling.

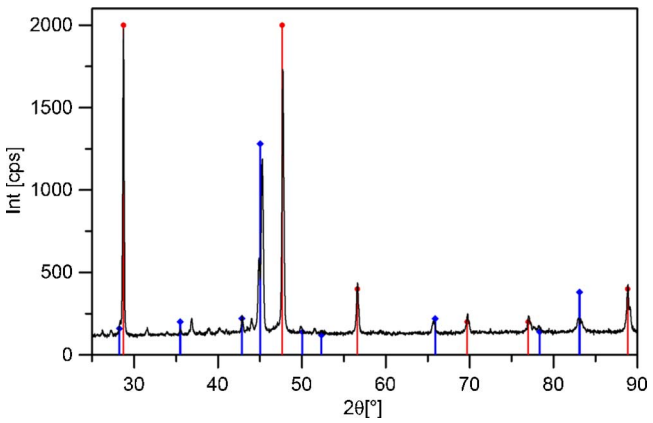

FIG. 7. XRD pattern of an Fe-Ni-Cu-Si- alloy bulk sample, showing two sets of peaks, η-Cu_3Si (blue, JCPDS 51–0916) and $NiSi_2$ (red, JCPDS 43–0989).

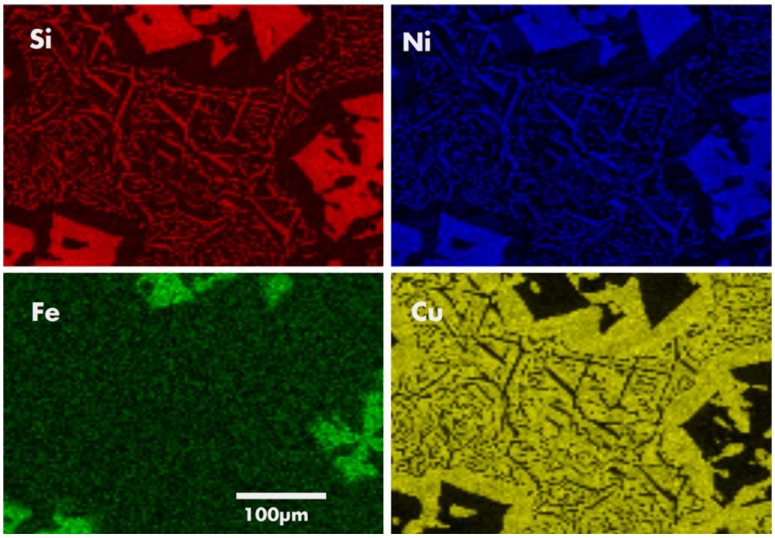

FIG. 8. EDS maps of a polished section of an Fe-Ni-Cu-Si alloy bulk sample showing $(Cu, Ni)_3Si$ and $(Ni, Cu, Fe)(Si, Cu)_2$ phases.

$NiSi_2$, but without phase speciation. The quenching apparently causes a freezing in early stages of precipitate formation before phase separation occurs. This shows that phase separation occurs at lower temperatures, which fits into our hypothesis that metal precipitates may be in a homogeneous or even liquid form at high temperatures, and then separate into several phases.

First results on Fe-Ni-Cu-Si alloy bulk samples confirm the coexistence of the same intermetallic phases like the ones found as precipitates in the silicon samples. Differential scanning calorimetry and a heating experiment confirmed that the Fe-Ni-Cu-Si- system contains compounds melting already at 740 °C.

The investigated intermetallic phases are of particularly significance for silicon, since their formation provides a local concentration of different transition metals in one spot, making them less harmful than in a homogeneously dissolved form. Further studies have to show how the concept of metal nanodefect engineering can be extended by using such precipitates as internal gettering centers.

ACKNOWLEDGMENTS

The authors thank V. Gottschalch for performing DSC measurements and J. Wu for preparing alloys. Professor Pizzini and his group at the University of Milano-Bicocca as well as P. Zang (UC Berkeley) are thanked for graciously providing us the as-grown, uncontaminated misfit dislocation structures for this investigation. This work was funded by the Deutsche Forschungsgemeinschaft within the project HE 3570/2-1 and NREL Subcontract AAT-2-31605-03. The operations of the Advanced Light Source at Lawrence Berkeley National Laboratory are supported by the Director, Office of Science, Office of Basic Energy Sciences, Materials Sciences Division, of the U.S. Department of Energy under Contract No. DE-AC03-76SF00098. Use of the Advanced Photon Source was supported by the U.S. Department of Energy, Office of Science, Office of Basic Energy Sciences, under Contract No. W-31-109-ENG-38. The authors acknowledge support of the National Center for Electron Microscopy, Lawrence Berkeley Laboratory, which is supported by the U.S. Department of Energy under Contract No. DE-AC02-05CH11231.

[1]R. M. Swanson, Prog. Photovolt. Res. Appl. **14**, 443 (2006).
[2]L. J. Geerligs, "Specification Of Solar Grade Silicon: How Common Impurities Affect The Cell Efficiency Of Mc-Si Solar Cells," presented at the 20th European Photovoltaic Solar Energy Conference and Exhibition, Barcelona, Spain, 6–10 June 2005), p. 619.
[3]A. A. Istratov, T. Buonassisi, M. D. Pickett, M. Heuer, and E. R. Weber, Mater. Sci. Eng., B **134**, 282 (2006).
[4]T. Buonassisi, A. A. Istratov, M. Heuer, M. A. Marcus, R. Jonczyk, J. Isenberg, B. Lai, Z. H. Cai, S. Heald, W. Warta, R. Schindler, G. Willeke, and E. R. Weber, J. Appl. Phys. **97**, 074901 (2005).
[5]S. A. McHugo, A. C. Thompson, A. Mohammed, G. Lamble, I. Perichaud, S. Martinuzzi, M. Werner, M. Rinio, W. Koch, H. U. Hoefs, and C. Haessler, J. Appl. Phys. **89**, 4282 (2001).
[6]T. Buonassisi, A. A. Istratov, M. A. Marcus, B. Lai, Z. H. Cai, S. M. Heald, and E. R. Weber, Nat. Mater. **4**, 676 (2005).
[7]D. Macdonald, A. Cuevas, A. Kinomura, Y. Nakano, and L. J. Geerligs, J. Appl. Phys. **97**, 033523 (2005).
[8]A. A. Istratov, T. Buonassisi, R. J. McDonald, A. R. Smith, R. Schindler, J. A. Rand, J. P. Kalejs, and E. R. Weber, J. Appl. Phys. **94**, 6552 (2003).
[9]M. Heuer, T. Buonassisi, M. A. Marcus, A. A. Istratov, M. D. Pickett, T. Shibata, and E. R. Weber, Phys. Rev. B **73**, 235204 (2006).
[10]T. Buonassisi, Acta Mater. (submitted).
[11]M. A. Marcus, A. A. MacDowell, R. Celestre, A. Manceau, T. Miller, H. A. Padmore, and R. E. Sublett, J. Synchrotron Radiat. **11**, 239 (2004).
[12]T. Buonassisi, A. A. Istratov, M. A. Marcus, M. Heuer, M. D. Pickett, B. Lai, Z. Cai, S. M. Heald, and E. R. Weber, Solid State Phenom. **108–109**, 577 (2005).
[13]O. F. Vyvenko, T. Buonassisi, A. A. Istratov, and E. R. Weber, J. Phys.: Condens. Matter **16**, S141 (2004).
[14]J. K. Solberg, Acta Crystallogr. A **34**, 684 (1978).